

# Stochastic Assembly of Two-Component Staphylococcal $\gamma$ -Hemolysin into Heteroheptameric Transmembrane Pores with Alternate Subunit Arrangements in Ratios of 3:4 and 4:3

Noriko Sugawara-Tomita, Toshio Tomita, and Yoshiyuki Kamio\*

Department of Molecular and Cell Biology, Graduate School of Agricultural Science, Tohoku University, Aoba-ku, Sendai 981-8555, Japan

Received 18 April 2002/Accepted 7 June 2002

**Self-assembling, pore-forming toxins from *Staphylococcus aureus* are illustrative molecules for the study of the assembly and membrane insertion of oligomeric transmembrane proteins. On the basis of previous studies, we have shown that the two-component  $\gamma$ -hemolysin assembles from LukF (or Hlg1, 34 kDa) and Hlg2 (32 kDa) to form ring-shaped transmembrane pores of ca. 200 kDa. Here we show that LukF and Hlg2 assemble in a stochastic manner to form alternate complexes with subunit stoichiometries of 3:4 and 4:3. High-resolution electron microscopic images of negatively stained pore complexes clearly revealed a heptameric structure. When adjacent monomers in the pore complexes were randomly cross-linked by using glutaraldehyde, LukF-LukF, LukF-Hlg2, and Hlg2-Hlg2 dimers were detected in an approximate ratio of 1:12:1, suggesting that LukF and Hlg2 were alternately arranged in the pore complex in molar ratios of 3:4 and 4:3. The alternate arrangements of LukF and Hlg2 in molar ratios of 3:4 and 4:3 were also visualized under electron microscope with the pore complexes consisting of glutathione *S*-transferase fusion protein of LukF or Hlg2 and wild-type protein of Hlg2 or LukF, respectively.**

Staphylococcal  $\gamma$ -hemolysin (Hlg), leukocidin (Luk), and Pantone-Valentine leukocidin (Luk-PV) are two-component cytolysins secreted by *Staphylococcus aureus*, a common pathogen in hospitals (5, 10, 19, 20). Hlg and Luk are illustrative molecules for the study of the assembly and membrane insertion of transmembrane proteins and have a unique characteristic of being composed of two separate water-soluble proteins (19). Hlg (Hlg1 of 34 kDa/Hlg2 of 32 kDa) effectively lyses erythrocytes from human and other mammalian species. Luk (LukF [34 kDa] and LukS [33 kDa]) is cytolytic toward human and rabbit polymorphonuclear leukocytes and rabbit erythrocytes (but not hemolytic toward human erythrocytes), and Luk-PV (LukF-PV [34 kDa] and LukS-PV [33 kDa]) reveals cytolytic activity with a high cell specificity to leukocytes. Previous studies by us and other groups showed that Hlg1 is identical to LukF and that the cell specificities of the cytolysins are determined by Hlg2 and LukS (2, 6, 17). Hence, Hlg1 is hereafter referred to as LukF in the present study. Based on the primary structures of the toxin components, Hlg, Luk, and Luk-PV are thought to form a family of proteins. Class F proteins (LukF and LukF-PV) and class S proteins (Hlg2, LukS, and LukS-PV) are ca. 70% identical to each other, whereas between classes the identity is ca. 30% (2, 13). Interestingly, class F and class S components of Hlg and Luk have 20 to 30% identities with the single-component staphylococcal  $\alpha$ -hemolysin (2), which has been intensively studied as a prototype of pore-forming cytolysins. Staphylococcal  $\alpha$ -hemolysin has been shown to assemble into ring-shaped heptamers pos-

sessing a transmembrane pore, whose three-dimensional structure was determined by X-ray crystallography (4, 14).

Because Hlg and Luk cause leakage of intracellular potassium ions from human and rabbit erythrocytes and swelling of the cells before hemolysis, we studied the assembly and pore-forming nature of these toxins (15, 16). (i) Assays of hemolytic activity in the presence of polyethylene glycols with different molecular sizes indicated that Hlg and Luk form membrane pores with functional diameters of 2.1 to 2.4 nm or 1.9 to 2.1 nm, respectively, in the target membranes. (ii) Electron microscopy of the toxin-treated erythrocytes revealed the presence of ring-shaped structures with outer and inner diameters of 9 and 3 nm, respectively, on the cells. (iii) Ring-shaped structures of the same dimensions were isolated from the toxin-treated erythrocytes or polymorphonuclear leukocytes after solubilization of the membranes with 2% sodium dodecyl sulfate (SDS) at 20°C and sucrose density gradient ultracentrifugation. (iv) SDS-polyacrylamide gel electrophoresis (PAGE) and Western blotting with specific antisera against the toxin components showed that the SDS-stable ring-shaped structures of Hlg and Luk were ca. 200-kDa complexes and contained two components in a molar ratio of 1:1. These results from analyses of populations of molecules implied that a single pore complex of Hlg and Luk may be a hexamer consisting of three molecules of each of two components. Later, Ferreras et al. reported that Hlg and Luk assembled into oligomers on the phosphatidylcholine-cholesterol liposomes and that hexamerization of the toxins was best fitted to the kinetics of vesicle permeabilization by Hlg and Luk (3). Thereafter, Olson et al. (11) and Pedelacq et al. (12) solved the crystal structures of the monomeric water-soluble forms of LukF and LukF-PV, respectively. These studies showed that LukF and LukF-PV have an almost identical structures with a fold of the membrane insertion domain and contain a core structure very similar to

\* Corresponding author. Mailing address: Department of Molecular and Cell Biology, Graduate School of Agricultural Science, Tohoku University, Aoba-ku, Sendai 981-8555, Japan. Phone: 81-22-717-8779. Fax: 81-22-717-8780. E-mail: ykamio@biochem.tohoku.ac.jp.

that of staphylococcal  $\alpha$ -hemolysin. On the basis of the crystal structures of the monomeric LukF and LukF-PV, Olson et al. constructed a model of the heptameric pores of the bicomponent cytolytins by using the  $\alpha$ -hemolysin heptamer as a template (11), whereas Pedelacq et al. proposed a hexameric structure for the transmembrane pores (12). Recently, Miles et al. reported that LukF and LukS of Luk form an octameric transmembrane pore (9). Their conclusion was based on the results obtained from gel shift electrophoresis and site-specific chemical modification during single-channel recording (9). Thus, the molecular architecture of the transmembrane pore of Hlg and Luk remains to be precisely elucidated. Is the complex hexameric, heptameric, or octameric? Does each ring-shaped complex contain both LukF and Hlg2? What is the molecular arrangement(s) of LukF and Hlg2 in the pore complexes?

Here we isolated transmembrane pore complexes of Hlg from human erythrocyte membranes, studied the stoichiometry of the pore complex, and determined the molecular arrangement of the two components by electron microscopy and chemical cross-linking. The results show that LukF and Hlg2 assemble into heteroheptameric pores with alternate arrangements of two components in molar ratios of 3:4 and 4:3.

#### MATERIALS AND METHODS

**Staphylococcal Hlg and hemolytic assay.** LukF and Hlg2 were purified from the culture supernatant of *S. aureus* 5R Smith strain and hemolytic assays were performed with human erythrocytes as described previously (15). Human erythrocytes ( $5 \times 10^7$  cells/ml) were incubated with LukF or Hlg2 at 37°C for 30 min, followed by the measurement of absorbance at 541 nm after centrifugation at  $800 \times g$  for 5 min. Protein concentration was assayed according to Bradford (1) with bovine serum albumin as a standard.

**Isolation of transmembrane pore complexes from erythrocyte membranes.** Ring-shaped pore complexes of LukF and Hlg2 were isolated as follows (15). Human erythrocytes ( $6 \times 10^{10}$  cells) were incubated with LukF (10  $\mu$ g/ml) and Hlg2 (10  $\mu$ g/ml) in 400 ml of Tris-buffered saline at 37°C for 30 min. Lysed erythrocytes were collected by centrifugation at  $22,000 \times g$  for 30 min at 4°C and were suspended in 100 ml of 5 mM Tris HCl buffer (pH 7.2), followed by centrifugation at  $22,000 \times g$  for 30 min at 4°C. Cell membranes of lysed erythrocytes thus obtained were packed by centrifugation with a Beckman SW55Ti rotor (Beckman Instruments, Inc., Palo Alto, Calif.) at 36,000 rpm for 1 h at 4°C and were solubilized with 2% (wt/vol) SDS at 20°C for 5 min. Under the conditions, the majority of Hlg pore complexes are not dissociated (15). The solubilized membranes were layered onto a 10 to 40% (wt/wt) sucrose linear gradient in 10 mM Tris HCl buffer (pH 7.2) containing 0.1% (wt/vol) SDS, which was centrifuged in a Beckman SW40 Ti rotor at 36,000 rpm for 15 h at 4°C. Distribution of the pore complexes was analyzed by SDS-PAGE as described by Laemmli (7), followed by Western blotting with specific antisera against LukF and Hlg2. Pore complexes sedimented faster than the membrane proteins of human erythrocytes in the sucrose gradient, and the major part of single pore complexes were recovered in the fractions of 15 to 20% sucrose, as shown previously (15, 16). The fractions containing pore complexes were concentrated by using an Amicon Centrifo YM-10 ultrafiltration membrane (Grace Co., Danvers, Mass.) and were further purified by the second sucrose gradient centrifugation as described above except for the use of a 10 to 30% (wt/wt) sucrose gradient. The fractions containing pore complexes were concentrated by using an Amicon Centrifo YM-10 ultrafiltration membrane and were dialyzed against 10 mM Tris HCl buffer (pH 7.2) containing 0.1% (wt/vol) SDS at 4°C.

**Electron microscopy of the transmembrane pore.** The purified pore complexes were placed onto a carbon-coated grid, washed briefly with 5 mM phosphate buffer (pH 7.2), and stained with 1% (wt/vol) sodium phosphotungstic acid (pH 7.2). Specimens were examined under a Hitachi electron microscope H-8100 (Hitachi Co., Tokyo, Japan) at an acceleration voltage of 100 kV. The same fields containing high-resolution images of ring-shaped pore complexes were photographed at 10 consecutive foci (i.e., from the just focus on the carbon film to under foci with 50-nm intervals). High-resolution images of pore complexes were collected from different fields and were printed with enlargement for analyzing the shape and the number of the subunit particles. The negative films were

further processed by optical filtering by using a Leica Quantimet 600 image analysis system (Leica Cambridge, Cambridge, England) to obtain the maximal contrast for the rings of toxin monomers.

**Immunoprecipitation of pore complexes with antibodies against LukF or Hlg2.** High-titer antisera against LukF and Hlg2 were raised in New Zealand White female rabbits, and the immunoglobulin G fractions were purified from the antisera as described previously (18). Unless otherwise stated, human erythrocytes ( $6 \times 10^9$  cells) were incubated with LukF (10  $\mu$ g/ml) and Hlg2 (10  $\mu$ g/ml) in 20 ml of Tris-buffered saline at 37°C for 30 min, and ring-shaped pore complexes were isolated as described above. Purified pore complexes were incubated with the antibodies against LukF or Hlg2 in an approximate molar ratio of 1:10 at 4°C for 15 h. Immunoprecipitates were heated at 100°C for 5 min and subjected to SDS-PAGE. Protein bands were stained with Coomassie brilliant blue R-250, and the intensity of the stained bands was determined by using Leica Quantimet 600 image analysis system.

**Cross-linking of pore complexes by glutaraldehyde.** The Hlg complexes were resistant to dissociation treatment with 2% SDS at 20°C but were broken into individual subunits upon treatment with 2% SDS at 100°C (15). Purified pore complexes (5 to 10  $\mu$ g of protein) were treated with 0.05% (vol/vol) glutaraldehyde at 20°C for 20 min. The glutaraldehyde-treated pore complexes were heated in the presence of 2% (wt/vol) SDS at 100°C for 5 min and subjected to SDS-PAGE on a 7% acrylamide gel. Protein bands in the gel were electroblotted onto a polyvinylidene difluoride sheet, followed by staining with Coomassie brilliant blue R-250 or by immunostaining with antiserum against LukF or Hlg2. The protein bands corresponding to 66-, 64-, and 62-kDa species were cut from the polyvinylidene difluoride sheet and analyzed for N-terminal amino acid sequences (8) by using an ABI model 491 protein sequencer (PE/Applied Biosystems, Foster City, Calif.).

**GST fusion proteins of LukF and Hlg2.** The *lukF* gene or the *hlg2* gene was amplified by a PCR with chromosomal DNA of *S. aureus* Smith 5R as a template. Amplified DNA fragments were digested with *EcoRI* and *XhoI* restriction endonucleases, and were inserted into the multicloning site of pGEX4T-1 (Pharmacia Biotechnol., Uppsala, Sweden). The resulting pGEX4T-1 plasmids (pGEX-LukF and pGEX-Hlg2), which carry *lukF* or *hlg2*, respectively, downstream of the glutathione *S*-transferase (GST) gene, were transformed into *Escherichia coli* BL21(DE3). The fusion proteins of LukF and Hlg2 (GST-LukF and GST-Hlg2, respectively) were produced and purified by using glutathione-Sepharose 4B (Pharmacia Biotech) as described by the manufacturer.

#### RESULTS AND DISCUSSION

**Two-component staphylococcal  $\gamma$ -hemolysin forms a heptameric transmembrane pore.** Transmembrane pore complexes of Hlg were purified from erythrocyte membranes of the toxin-treated cells by a procedure including solubilization of erythrocyte membranes with 2% SDS at 20°C and separation of the pore complexes from the membrane proteins of human erythrocytes by using two steps of sucrose gradient centrifugation. The major portion of ring-shaped pore complexes of Hlg are resistant to the dissociation treatment with 2% SDS at 20°C (15, 16). Although clusters of the pore complexes were also recovered from the toxin-treated erythrocyte membranes upon the treatment with 2% SDS at 20°C, they were separated from single pore complexes by the two steps of sucrose gradient centrifugation, as shown previously (15, 16). The preparations of single pore complex thus obtained were stained with sodium phosphotungstic acid and were subjected to electron microscopy. As shown in Fig. 1A, we observed many single rings with outer and inner diameters of 9 and 3 nm, respectively, and a few striped rectangles with widths of 9 and 10 nm (arrows indicate the rectangles in Fig. 1A) in the specimens. The rings represented the top views of a hollow cylindrical structure of pore complex, and the striped rectangles represent the side view of a pore complex. These results showed that an Hlg transmembrane pore had a hollow cylindrical structure with outer and inner diameters of 9 and 3 nm, respectively, and with a height of 10 nm. High-resolution images of the ring-shaped

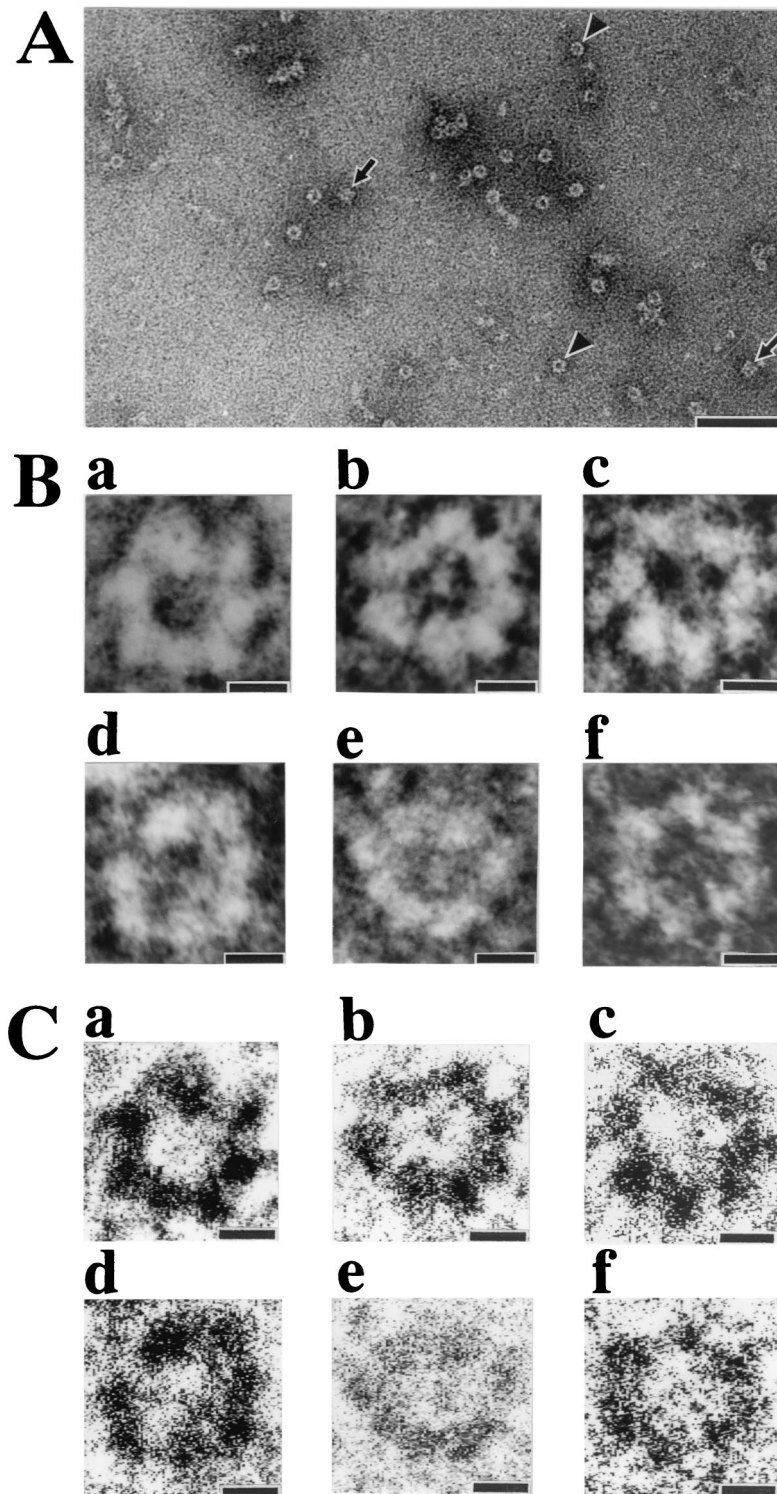


FIG. 1. Electron microscopic images of negatively stained transmembrane pores of Hlg (A), high-resolution images of the pore complexes (B), and contrast-enhanced high-resolution images of the same pore complexes shown in panel B (c). (A) Pore complexes isolated from toxin-treated human erythrocytes were stained with 1% (wt/vol) sodium phosphotungstic acid and were subjected to electron microscopy as described in Materials and Methods. Arrowheads and arrows indicate the top views (the ring-shaped structures) and the side views of the pore complexes, respectively. Bars, 50 nm. (B) High-resolution ring-shaped images (top views) of the pore complex in different fields were collected and enlarged. Bars, 3 nm. (C) The same ring-shaped structures shown in panel B were contrast enhanced by using a Leica Quantimet 600 image analysis system. Bars, 3 nm.

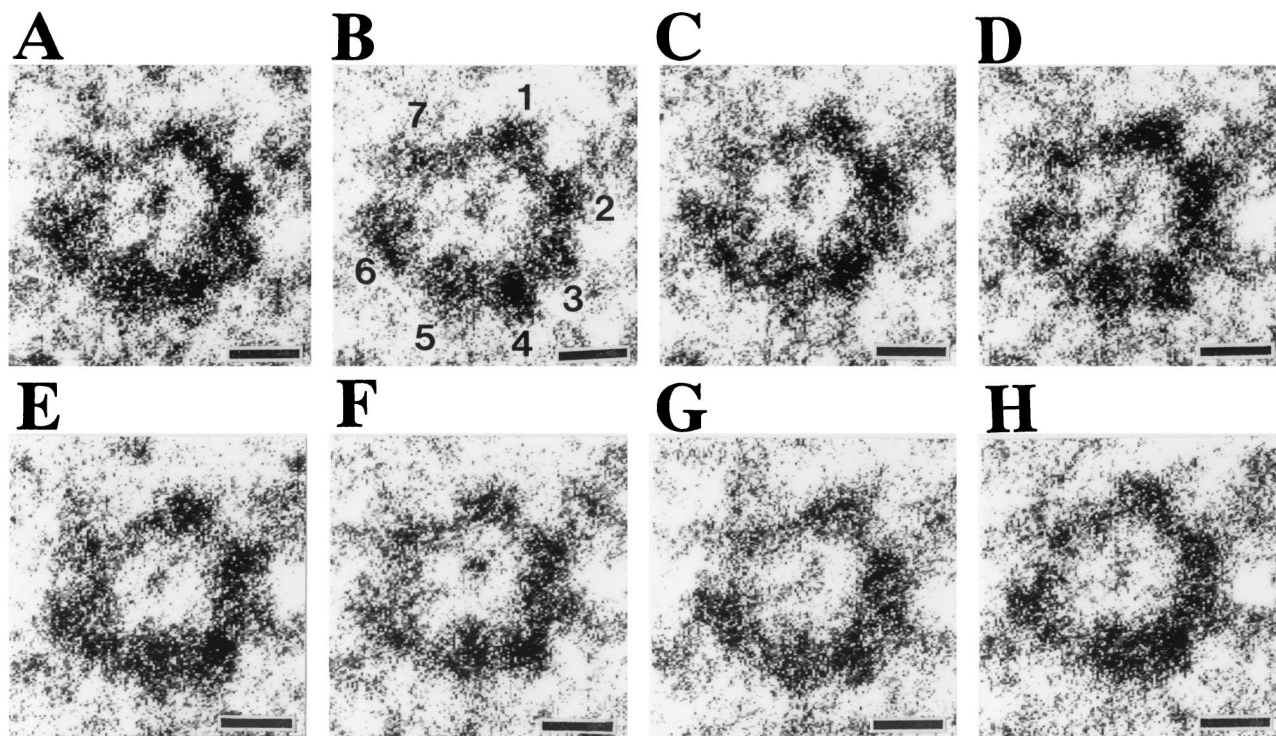


FIG. 2. High-resolution images for the same pore complex taken at eight consecutive foci. Electron micrographs for the fields containing high-resolution images of the ring-shaped structure of pore complexes were taken at eight consecutive foci as described in Materials and Methods. A set of the consecutive images for the same ring is shown in panels A to H. In panel B, seven distinguishable particles were numbered. Bars, 3 nm.

structures were collected from many fields of the electron micrographs (arrowheads indicate such high-resolution images of the pore complexes in Fig. 1A), and were enlarged to count the number of particles (subunits) in each ring. As shown in Fig. 1B, seven particles of a similar size were clearly visible in the rings of the pore complexes. To better resolve individual subunits in the ring-shaped structures, negatively stained images of the pore complexes were optically filtered by using a Leica Quantimet 600 image analysis system (Fig. 1C). The processed images of the pore complexes clearly revealed seven particles in the ring-shaped structures (Fig. 1C).

To determine the subunit stoichiometry of the Hlg transmembrane pore, we attempted to count the number of particles in a ring for more than 150 pore complexes. Images of the negatively stained specimen pore complexes were taken at eight consecutive foci with 50-nm intervals, and high-resolution images of ring-shaped structures were selected from different fields and subjected to optical filtering by using a Leica Quantimet 600 image analysis system. Figure 2 shows a set of eight contrast-enhanced consecutive images for the same ring-shaped structure, which has been shown in Fig. 1Bb and Cb as a representative heptameric structure. Seven particles of a similar size are clearly visible in Fig. 2B, which was taken at 50 nm under focus relative to the surface of carbon film. However, some particles were not as well resolved: (i) two particles (i.e., the no. 2 and the no. 3 particles; numbered according to Fig. 2B) were fused in Fig. 2G, giving an apparent hexameric structure, and (ii) eight particles were visible in Fig. 2C, where a

particle (i.e., the no. 7 particle) appeared to be split into two smaller particles. Ring-shaped structures of pore complexes, whose individual subunits had a similar size in the contrast-enhanced images, were randomly collected from different fields, and the number of particles in each ring was counted for 179 rings by comparing the images of the same rings taken at eight consecutive foci. As a result, 139 (78%) rings of 179 pore complexes revealed a heptameric structure, whereas 30 (17%) and 10 (5%) rings appeared to have six or eight particles, respectively. We therefore conclude that the Hlg transmembrane pore has a heptameric stoichiometry. The hexameric and the octameric structures of the pore complex would be due, at least in part, to a merged image of two adjacent subunits and a splitting of a single subunit to two parts, respectively, in the electron microscopic images. Alternatively, a small portion of the rings would have a hexameric, or an octameric structure. Incidentally, we failed to clearly enhance a heptagonal arrangement of the Hlg subunits for the images of the rings of Fig. 1B when we tentatively determined the centers of the heptameric rings and rotated the images (results not shown). Thus, we determined the centers for each of the subunit particles and measured the angles between two adjacent particles. The measurement showed that the ring-shaped heptamers have a range of angles between 60 and 40° (i.e., the ring of Fig. 1Bb has angles of 59.5, 57.5, 53.5, 52.5, 48.1, 46.5, and 42.4°, and the ring of Fig. 1Bc has angles of 60.7, 59.8, 53.5, 49.5, 48.8, 48.2, and 39.5°). Deformation of the rings could have occurred, at least in part, during the preparation of the specimens, which

may reflect an inherent fragility of the pore complexes, possibly due to the asymmetric heteroheptameric arrangements of LukF and Hlg2 (see below).

**Heptameric transmembrane pore of Hlg has alternate arrangements of LukF and Hlg2 components in molar ratios of 3:4 and 4:3.** Our previous studies showed that populations of the isolated pore complexes of Hlg contained LukF and Hlg2 in an approximate molar ratio of 1:1, when human erythrocytes were incubated with LukF and Hlg2 of an equal concentration (15, 16). The molar ratio of LukF to Hlg2 in the isolated pore complexes remained 1:1 when the molar ratio of LukF to Hlg2 was changed to 2:1 or 1:2 in the incubation with human erythrocytes (results not shown). Furthermore, immunoprecipitation experiments for the isolated pore complexes showed that each of the antiserum against LukF or Hlg2 precipitated the pore complexes consisting of LukF and Hlg2 in an approximate molar ratio of 1:1 (results not shown). These results suggested that a heptameric pore complex contained both of LukF and Hlg2, in an average molar ratio of 1:1.

To elucidate the molecular arrangements of LukF and Hlg2 in the heptameric pore complex, adjacent subunits in the complex were cross-linked by glutaraldehyde under conditions in which production of cross-linked dimers was optimized (as described in Materials and Methods). The glutaraldehyde-treated pore complexes were treated with 2% SDS at 100°C to dissociate non-cross-linked adjacent subunits, followed by SDS-PAGE and staining with either Coomassie brilliant blue R-250 or antiserum to LukF or Hlg2. As shown in Fig. 3A (first and second lanes), the bands corresponding to 66 and 64 kDa were immunostained with antiserum against LukF, whereas the bands corresponding to 64 and 62 kDa were immunostained with anti-Hlg2 serum. N-terminal amino acid sequencing for these protein bands indicated that the N-terminal 10 amino acid residues of the proteins of 66 and 62 kDa were identical to those of LukF and Hlg2, respectively. In contrast, the protein band corresponding to 64 kDa corresponded to the N-terminal 10 amino acid residues of both LukF and Hlg2 in an approximate molar ratio of 1:1 (Fig. 3B). These results clearly showed that the protein bands corresponding to 66, 64, and 62 kDa were LukF homodimer, LukF-Hlg2 heterodimer, and Hlg2 homodimer, respectively, and that heterodimeric arrangement of LukF and Hlg2 was predominant in the heptameric pore complexes. Furthermore, relative intensities of the Coomassie brilliant blue R-250-stained bands corresponding to 66, 64, and 62 kDa were measured by densitometry, and an averaged ratio among the relative intensities of the bands was obtained from five independent experiments. The densitometry for the protein bands corresponding to 66, 64, and 62 kDa gave relative intensities in an approximate ratio of 1:12:1 (Fig. 3C). The densitometry for the protein bands also indicated that ca. 50% of the monomers were cross-linked by glutaraldehyde under these conditions (results not shown). These results showed that LukF and Hlg2 are alternately arranged in the heptameric pore complexes and that, on average, pore complexes contained LukF-LukF, LukF-Hlg2, and Hlg2-Hlg2 linkages in a ratio of 0.5:6.0:0.5. On the assumption that two adjacent subunits in the pore complex were randomly cross-linked with equal frequency, we calculated the probabilities of the formation of LukF-LukF, LukF-Hlg2, and Hlg2-Hlg2 dimers for each of the possible heteroheptamers (Fig. 4).

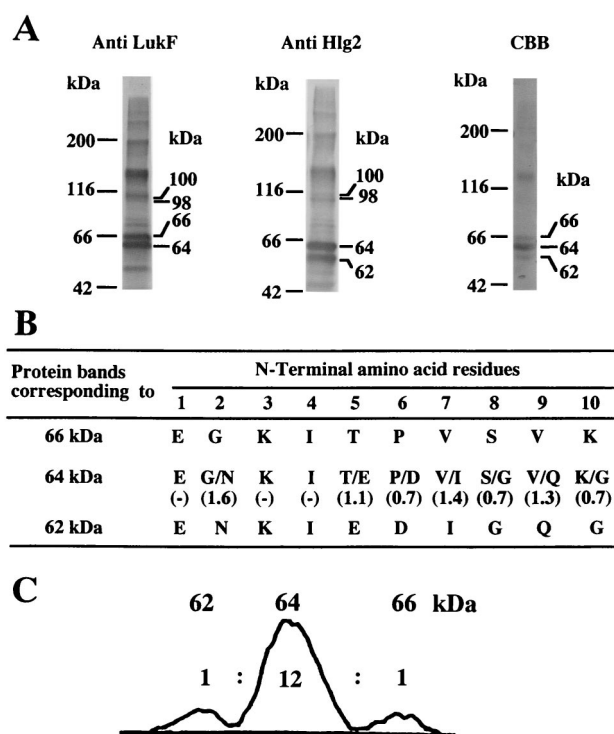


FIG. 3. Cross-linking of adjacent subunits in the pore complex and analysis of cross-linked dimers. (A) Purified pore complexes (ca. 10  $\mu$ g of protein) were treated with 0.05% (vol/vol) glutaraldehyde at 20°C for 20 min, heated at 100°C in the presence of 2% SDS, and subjected to SDS-PAGE with a 7% acrylamide gel. Protein bands in the gel were electroblotted to a polyvinylidene difluoride sheet, followed by immunostaining with antiserum against LukF or Hlg2 (lanes 1 and 2, respectively) or staining with Coomassie brilliant blue R-250 (lane 3). (B) The N-terminal 10 amino acid residues and relative molar ratios of amino acid residues at the same positions were determined for the protein bands corresponding to 66, 64, and 62 kDa. (C) Relative intensities of the Coomassie brilliant blue R-250-stained bands corresponding to 66, 64, and 62 kDa were measured for lane 3 by using Leica Quantimet 600 image analysis system.

We also summed the probabilities of the dimer formation for each of the combinations of heteroheptamers with subunit ratios of 6:1 and 1:6 (type A), 5:2 and 2:5 (types B to D), and 4:3 and 3:4 (types E to I) (Fig. 4). As shown in Fig. 4, only the combination of alternate arrangements of LukF and Hlg2 in molar ratios of 3:4 and 4:3 (type I) can interpret the formation of LukF-LukF, LukF-Hlg2, and Hlg2-Hlg2 dimers in an approximate molar ratio of 1:12:1. In contrast, all other combinations of heteroheptamers (types A to H) should produce LukF-LukF, Hlg2-Hlg2, and LukF-Hlg2 in molar ratio of 1:1:0.8 or 1:1:2.67 (Fig. 4). In addition, when all of the possible heteroheptamers were formed in an equal frequency (i.e., LukF and Hlg2 are randomly arranged in the rings), LukF-LukF, Hlg2-Hlg2, and LukF-Hlg2 dimers should be detected in an approximate ratio of 1:1:2 (Fig. 4). Thus, heptameric transmembrane pores of Hlg may have two alternate arrangements of LukF and Hlg2 in molar ratios of 3:4 and 4:3, and the two types of pore complexes may be formed in an equal frequency.

Besides the bands for toxin dimers, we also detected immunostained bands corresponding to ca. 100 and 130 kDa (Fig. 3A), which probably correspond to the bands for trimers and



















Probabilities of the formation of LukF-LukF (●●), Hlg2-Hlg2 (○○), and LukF-Hlg2 (●○)			
Type	For each of heteroheptamers		For each type
A	 15:0:6	 0:15:6	15:15:12
B	 12:3:6	 3:12:6	15:15:12
C	 9:0:12	 0:9:12	9:9:24
D	 9:0:12	 0:9:12	9:9:24
E	 9:6:6	 6:9:6	15:15:12
F	 6:3:12	 3:6:12	9:9:24
G	 6:3:12	 3:6:12	9:9:24
H	 6:3:12	 3:6:12	9:9:24
I	 3:0:18	 0:3:18	3:3:36
For total types (A-I)		93 : 93: 192	

FIG. 4. Probabilities of the formation of LukF-LukF, Hlg2-Hlg2, and LukF-Hlg2 dimers by random cross-linking with glutaraldehyde. Relative probabilities of the formation of LukF-LukF (●●), Hlg2-Hlg2 (○○), and LukF-Hlg2 (●○) dimers by random cross-linking are presented as ratios of LukF-LukF to Hlg2-Hlg2 to LukF-Hlg2 (●●:○○:●○) for each of the possible heteroheptamers, for each of combination of the heteroheptamers with subunit ratios of 6:1 and 1:6 (type A), 5:2 and 2:5 (types B to D), and 4:3 and 3:4 (types E to I), and for the total of the possible heteroheptamers.

tetramers of toxin component(s). Two bands corresponding to 100 and 98 kDa were immunostained with both of antisera against LukF and Hlg2 (Fig. 3A, lanes 1 and 2), and the upper band corresponding to 100 kDa was more intensely stained with anti-LukF serum (Fig. 3A, lane 1), whereas the lower band corresponding to 98 kDa was more intensely stained with anti-Hlg2 serum (Fig. 3A, lane 2). Thus, the treatment of pore complexes with glutaraldehyde produced heterotrimers (LukF)2Hlg2 and LukF(Hlg2)2 (whose molecular sizes are calculated to be 100 and 98 kDa, respectively) but no homotrimer of LukF and Hlg2 (whose molecular sizes are calculated to be 102 and 96 kDa, respectively). These results are consistent with alternate arrangements of LukF and Hlg2 in molar ratios of 3:4 and 4:3, because cross-linking for the 3:4 and 4:3 heteroheptamers by glutaraldehyde should produce an equal amount of (LukF)2Hlg2 and LukF(Hlg2)2 species. Furthermore, cross-linking for the heteroheptamers by glutaraldehyde should produce (LukF)3Hlg2, (LukF)2(Hlg2)2, and LukF(Hlg2)3 (whose molecular sizes are calculated to be 134, 132, and 130 kDa, respectively) in a ratio of 1:5:1. In fact, a broad

band corresponding to 120 to 130 kDa was immunostained with antisera against LukF and Hlg2 (Fig. 3A), suggesting that the broad band may contain multiple types of heterotetramer. However, because of the limited resolution on the SDS-PAGE with a 7% acrylamide gel, the individual heterotetrameric complexes could not be resolved. Incidentally, the broad band corresponding to 120 to 130 kDa was much more intensely stained with Coomassie brilliant blue R-250 than the bands corresponding to 98 and 100 kDa in Fig. 3A. However, ratio of the integrated intensity for the bands corresponding to 120 to 130 kDa to that for the bands corresponding to 98 to 100 kDa was in the range of 1.5 to 1.0 in the other four experiments (results not shown).

**Visualization of alternate arrangements of LukF and Hlg2 in the heptameric pore complexes.** To visualize the arrangements of LukF and Hlg2 in the pore complex, we constructed a GST fusion protein of LukF (GST-LukF) and used it together with wild-type protein of Hlg2 to form GST-tagged pore complexes for electron microscopy. X-ray crystallography for monomeric LukF showed that the N terminus of LukF is exposed at the protein surface and that it is located in the site opposite to the putative stem domain that may be inserted into the cell membrane to form the transmembrane pore (11, 12). Therefore, the GST portion of the fusion protein was expected to not hinder assembly of GST-LukF into functional pore complex, and it may be observed as a tag protruding from the ring-shaped structure. In fact, the constructed GST-LukF exhibited hemolytic activity as high as wild-type LukF in the presence of Hlg2, and the ring-shaped structures with outer and inner diameters of 9 and 3 nm, respectively, were observed on the surface of toxin-treated erythrocytes (results not shown). After solubilization of the toxin-treated erythrocyte membranes with 2% (wt/vol) SDS, the pore complexes of GST-LukF and Hlg2 were purified by sucrose gradient centrifugation, stained with 1% sodium phosphotungstic acid, and subjected to electron microscopy. As shown in Fig. 5, ring-shaped structures were associated with four or three ellipsoidal particles (i.e., probably the GST portion of GST-LukF molecules) possessing the major axis of 4 to 6 nm. In the rings carrying four particles (Fig. 5A-5C), no or one subunit seemed to be situated between the positions of two GST-LukF subunits. In contrast, one or two subunits were expected to be present between the positions of GST-LukF subunits in the rings carrying three particles (Fig. 5D to F). Thus, the positions of GST-LukF in the rings were found to meet the expected positions of GST-LukF in the alternate arrangements of LukF and Hlg2 in ratios of 4:3 or 3:4.

To visualize the positions of Hlg2 molecules in the ring-shaped complex, the GST fusion protein of Hlg2 (GST-Hlg2) was constructed. The constructed GST-Hlg2 exhibited hemolytic activity as high as that of wild-type Hlg2 in the presence of LukF (results not shown). Ring-shaped complexes were isolated from the membranes of human erythrocytes, stained with sodium phosphotungstic acid, and analyzed by electron microscopy. High-resolution images of the ring-shaped complexes revealed particular subunits with or without a protrusion (Fig. 6Aa, Ba, and Ca). To better resolve individual subunits in the rings, the negatively stained images were optically filtered by using a Leica Quantimet 600 image analysis system (Fig. 6Ab, Bb, and Cb), and individual subunit particles in the contrast-

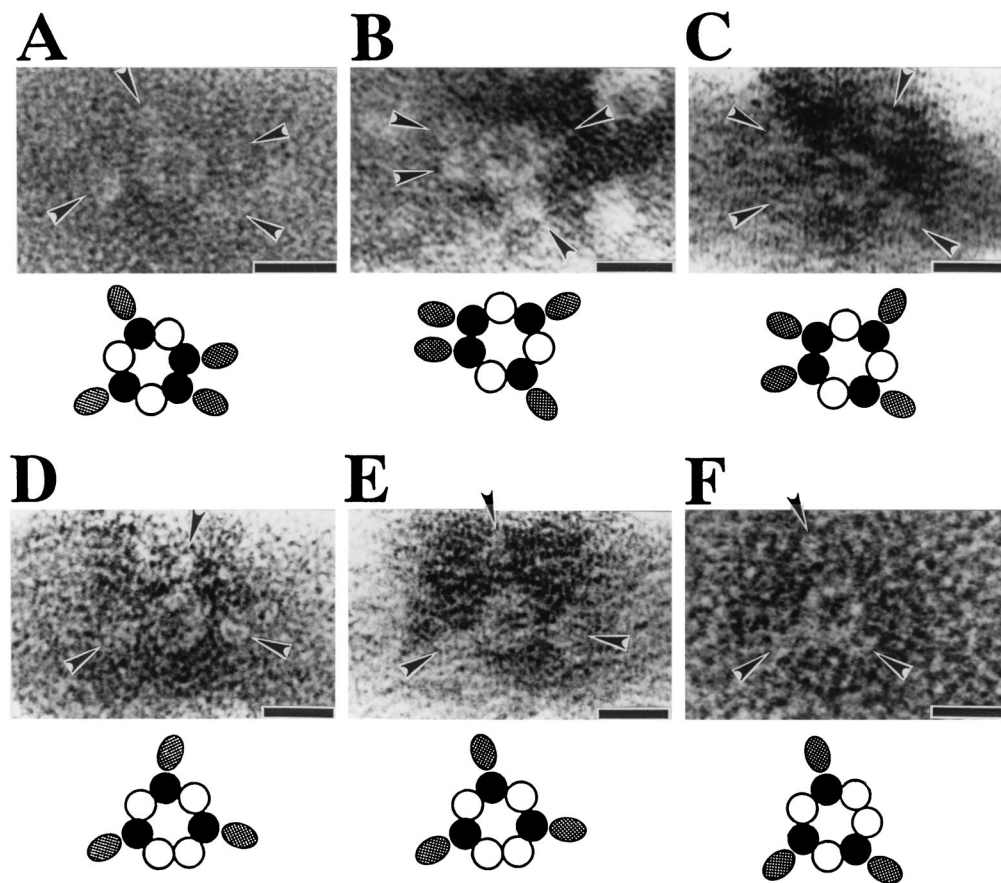


FIG. 5. Visualization of the molecular arrangement of LukF and Hlg2 in the pore complex by use of GST fusion proteins of LukF. Pore complexes consisting of GST-LukF and Hlg2 were isolated from human erythrocyte membranes as described in Materials and Methods, except that GST-LukF was used at a concentration of 19  $\mu\text{g/ml}$  instead of at 10  $\mu\text{g/ml}$ . Purified pore complexes were stained with 1% (wt/vol) sodium phosphotungstic acid and were tested under an electron microscope. The ellipsoidal particles, which are indicated by arrowheads, may correspond to the GST part of GST-LukF. Note that the arrowheads are directed to GST-LukF in the alternate arrangements, which are illustrated below. In the illustrations, closed and open circles indicate LukF and Hlg2, respectively, and ellipses indicate the GST part of GST-LukF. Bars, 10 nm.

enhanced images were traced (Fig. 6Ac, Bc, and Cc). Figure 6A shows a ring consisting of seven subunit particles, and three of the particles had a protrusion. In the ring, one or two particles without protrusion were observed between the particles with a protrusion (Fig. 6A). Figure 6B and C showed the rings consisting of seven subunits, of which four subunits had protrusions. In these rings, one subunit without protrusion was observed between the subunits with the protrusion (Fig. 6B and C). Furthermore, three upward protrusions with length of ca. 9 nm were observed in the side view of a ring-shaped complexes of LukF and GST-Hlg2 (Fig. 7A), whereas such a protrusion was not visible in the side view of the pore complex consisting of LukF and Hlg2 (Fig. 7B, i.e., an enlarged image of the striped rectangle shown in Fig. 1A). These results indicated that the protrusions from subunit particles correspond to the GST portions of GST-Hlg2. Taken together, the images of the ring-shaped complexes shown in Fig. 6 are consistent with the alternate arrangements of LukF and Hlg2 in ratios of 4:3 or 3:4. The upward protrusion of the GST portion (Fig. 7) suggests flexibility of the N-terminal part of Hlg2 molecule, which may cause the different-shaped GST protrusions in the images of the pore complexes (Fig. 6), and the extended GST domain

of the GST-Hlg2 may be formed by the treatment of the rings with 2% SDS in the isolation procedure.

In this study, we showed that Hlg assembles into heteroheptameric transmembrane pores with alternate arrangements of the two components in molar ratios of 3:4 and 4:3. Formation of two types of heteroheptamers would start from alternate assembly of LukF and Hlg2 into an open-circular heterohexamers, followed by binding of either LukF or Hlg2 to its distal counterpart and subsequent linkage between homologous monomers (Fig. 7). The formation of a homodimeric entity in the heteroheptameric pore complex is quite feasible on the basis of the following evidence (N. Sugawara et al.; unpublished observations). First, when LukF and Hlg2 were used at high concentrations, each of the Hlg components assembled into ca. 200-kDa pore complexes in the absence of its counterpart and lysed human erythrocytes. LukF and Hlg2 cooperatively lysed 50% of the human erythrocytes at concentrations of 0.3  $\mu\text{g/ml}$  for each of the components, whereas LukF and Hlg2 induced 50% hemolysis at concentrations of 50 and 30  $\mu\text{g/ml}$ , respectively, in the absence of their counterpart. Second, electron microscopy for the erythrocytes lysed by single components showed the presence of ring-shaped structures with

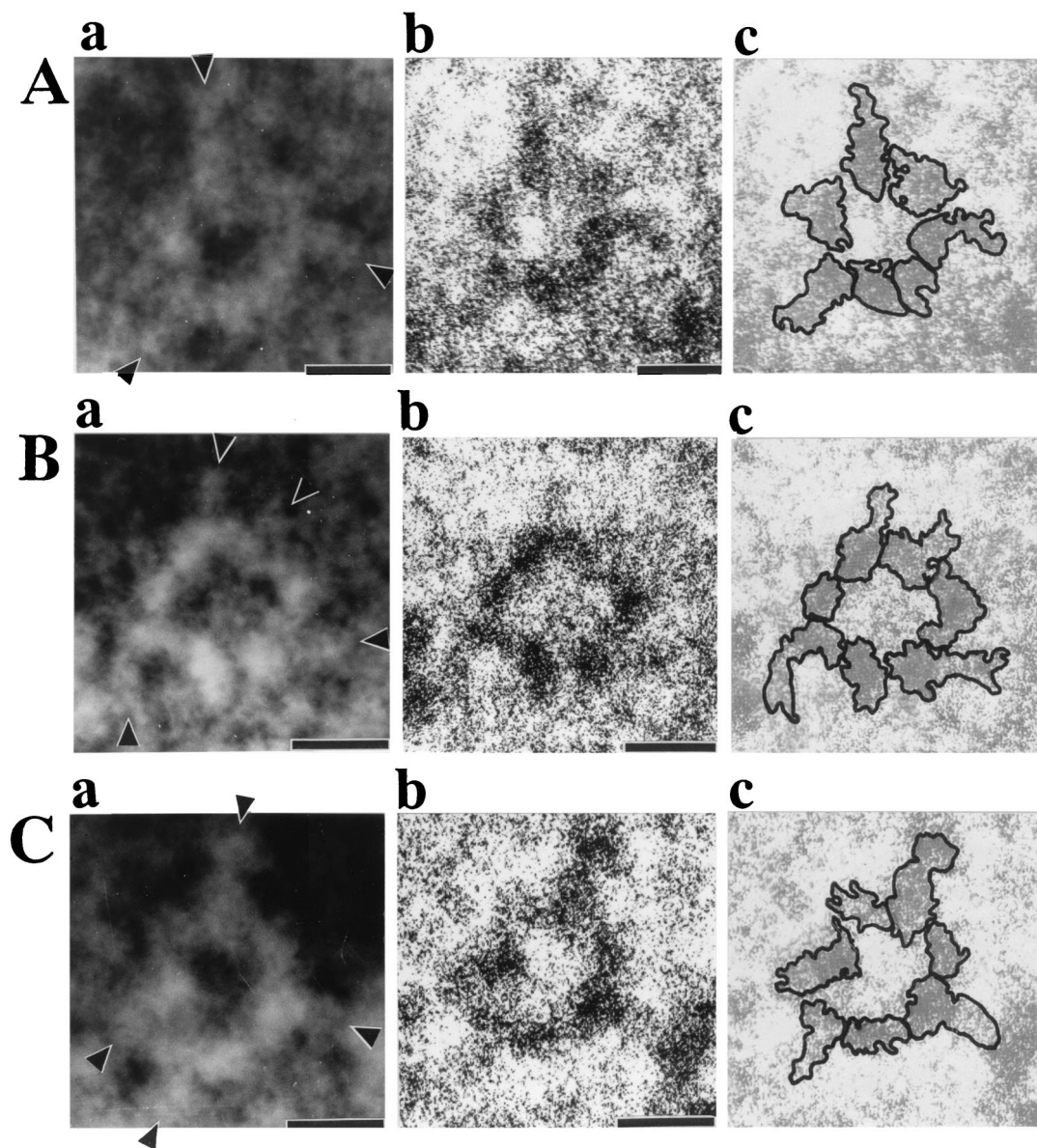


FIG. 6. Visualization of the molecular arrangement of LukF and Hlg2 in the pore complex by use of GST-Hlg2. Pore complexes consisting of GST-Hlg2 and LukF were isolated and subjected to electron microscopy as described in the legend for Fig. 5. High-resolution images of the ring-shaped complexes are shown in panels Aa, Ba, and Ca. The negatively stained images were contrast enhanced by optical filtering with a Leica Quantimet 600 image analysis system (Ab, Bb, and Cb), and the outlines of individual subunit particles were traced in the contrast-enhanced images (Ac, Bc, and Cc). Bars, 5 nm.

outer and inner diameters of 9 and 3 nm, respectively, although fewer of the ring-shaped structures were observed per cell compared to that seen on the erythrocytes lysed by the two components. Ring-shaped homooligomeric complexes of LukF and Hlg2 were isolated from the toxin-treated erythrocytes, and the dimensions of the homooligomers were similar to those of the heteroheptameric pores. Third, the functional diameters were estimated to be ca. 2 nm for the homomeric transmembrane pores consisting of LukF or Hlg2. These results suggest that homologous subunits were linked to form ring-shaped pore complexes of the same dimensions as the heteroheptameric pores, although linkages between LukF and

Hlg2 may be formed much more efficiently than those linkages between identical subunits. Therefore, open-circular heteroheptamer of LukF and Hlg2 would be closed through linkage between homologous monomers. This mechanism explains the formation of equal amounts of 3:4 and 4:3 heteroheptamers of LukF and Hlg2 (Fig. 8). Generally, subunit stoichiometry is strictly determined for the functional multicomponent supermolecules of biological systems, so the formation of two types of transmembrane pores is a unique characteristic of Hlg. It remains to be studied how Hlg assembles in a stochastic manner to form the 3:4 and 4:3 heteroheptamers on the target cells and whether two types of transmembrane pores have func-



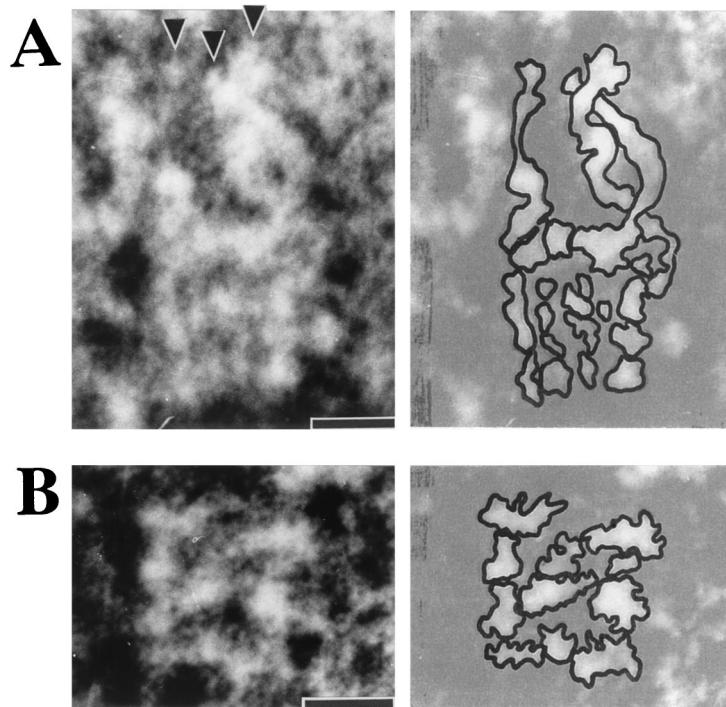


FIG. 7. Side views of the ring-shaped complexes consisting of LukF and GST-Hlg2 (A) or LukF and Hlg2 (B). Negatively stained images for a side view of the pore complex consisting of LukF and GST-Hlg2 (A) or consisting of LukF and Hlg2 (B) are shown, and the outlines of the side views are traced. Note that the ring containing GST-Hlg2 has three protrusions of ca. 9 nm in an upward direction. Arrowheads indicate the protrusions. Bars, 5 nm.

tional differences, such as different channeling activities to small ions.

With respect to the biological significance of the heteroheptameric pore of Hlg, we have recently found that the heteroheptamers of Hlg form clusters on human erythrocytes to enhance hemolysis (N. Sugawara-Tomita et al., unpublished data). (i) Electron microscopy of the Hlg-treated erythrocytes revealed that Hlg formed clusters of pore complexes, as well as

single pore complexes on the cells, and that the cell membrane was prominently disrupted in areas surrounding the clusters, in which many (i.e., 60 to 80) pore complexes were piled up. (ii) Direct counting for average numbers of the pore complexes per unit area of cell membrane under the electron microscope showed that cluster formation of the pore complexes occurred in tandem with hemolysis of human erythrocytes upon exposure of the cells to lower doses of the toxin, whereas the formation of single pore complexes more strongly correlated with the swelling of the cells. Thus, clustering of the pore complexes would cause an intensive damage of cell membrane in the limited areas, leading to enhancement of hemolysis, and the cluster-forming ability of the pore complexes may be due to the asymmetric heteroheptameric architecture, including the homodimeric linkage.

Miles et al. have recently proposed an octameric structure for the transmembrane pore of Luk on the basis of the results obtained from gel shift electrophoresis and site-specific chemical modification during single-channel recording (9). Because they failed to count all of the subunits at once in a single experiment of gel shift electrophoresis with the fusion proteins of LukF and LukS with a C-terminal extension of 94 amino acid residues, they separately counted LukF and LukS in different experiments with one of the fusion proteins. Thus, the maximal numbers of LukF and LukS in a single pore complex were determined to be four for both the components, but the total number of the subunits was not determined. For counting the subunits by the lipid bilayer experiments, Miles et al. incorporated the pore complexes composed of cysteine-substi-

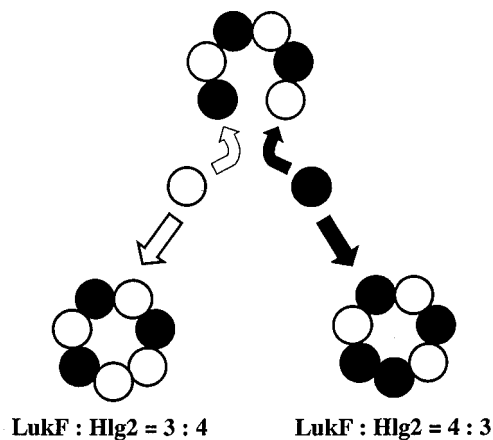


FIG. 8. A possible model of stochastic assembly of LukF and Hlg2 into 3:4 and 4:3 heteroheptamers. LukF and Hlg2 assemble into an open-circular heterohexamer (LukF-Hlg2)<sub>3</sub>, followed by binding of either LukF (●) or Hlg2 (○) to its distal counterpart and subsequent linkage between homologous subunits.

tuted LukF and LukS (i.e., LukF-S124C and LukS-A122C) into the bilayer membranes of diphytanoyl phosphatidylcholine and measured the stepwise decrease in the current by the site-specific chemical modification with a sulfhydryl-specific reagent, sodium (2-sulfonatoethyl)methanethiosulfonate. In the single-channel recordings, these authors observed four steps in eleven recordings and three steps in one recording with pore complexes composed of LukF-S124C and wild-type LukS and observed four steps in all of nine recordings with pore complexes containing wild-type LukF and LukS-A122C. In contrast, with pore complexes containing both LukF-S124C and LukS-A122C, Miles et al. observed seven steps in one recording, six steps in four recordings, and five steps in one recording. Again, the separate counting for the maximal numbers of LukF and LukS subunits favored the octameric stoichiometry, but it was difficult to count all of the subunits at once. It should be noted that their results are also consistent with the heptameric stoichiometry with 3:4 and 4:3 compositions of LukF and LukS. It seems likely that Luk and Hlg form the pore complexes with the same subunit stoichiometry, because of their similar size and morphology, estimated from electron microscopy and osmotic protection experiments (15, 16). Thus, further study is needed for counting the total number of subunits in the pore complex of Luk. Compared with the study of Miles et al. (9), an advantage of this study is the use of electron microscopy, by which we were able to count directly the subunits in the pore complexes at once (Fig. 1B). Further, the results obtained from the cross-linking experiments clearly demonstrated the alternate arrangements of LukF and Hlg2, and all of the results of the cross-linking experiments and the electron microscopy with GST fusion proteins of LukF and Hlg2 were consistent with the 3:4 and 4:3 heteroheptameric structures with alternate arrangements. However, if the pore complexes of Hlg have a three-dimensional structure similar to that of staphylococcal  $\alpha$ -hemolysin, cross-links between non-neighboring subunits cannot be excluded totally in the pore complexes of Hlg because the N-terminal latch of staphylococcal  $\alpha$ -hemolysin stretches as far as subunit  $n+2$  (i.e., the subunit next to the nearest neighbor) in the crystal structure of the pore complex (14). To confirm the 3:4 and 4:3 heteroheptameric structures of Hlg transmembrane pores, we are currently visualizing the total number and the molecular arrangement of LukF and Hlg2 in the pore complex by using the gold-labeled GST fusion proteins of the two components.

#### ACKNOWLEDGMENTS

This work was supported in part by a Grant-in-Aid for Scientific Research from the Ministry of Education, Science, Sports, and Culture of Japan. N.S.-T. is a recipient of a postdoctoral fellowship from the Japan Society for the Promotion of Science.

#### REFERENCES

- Bradford, M. M. 1976. A rapid and sensitive method for the quantitation of microgram quantities of protein utilizing the principle of protein-dye binding. *Anal. Biochem.* **72**:248–254.
- Cooney, J., Z. Kienle, T. J. Foster, and P. W. O'Toole. 1993. The gamma-hemolysin locus of *Staphylococcus aureus* comprises three linked genes, two of which are identical to the genes for the F and S components of leukocidin. *Infect. Immun.* **61**:768–771.
- Ferreras, M., F. Hoepfer, M. D. Serra, D. A. Colin, G. Prevost, and G. Menestrina. 1998. The interaction of *Staphylococcus aureus* bi-component  $\gamma$ -hemolysins and leukocidins with cells and lipid membranes. *Biochim. Biophys. Acta* **1414**:108–126.
- Gouaux, J. E., O. Braha, M. R. Hobaugh, L. Song, S. Cheley, C. Shustak, and H. Bayley. 1994. Subunit stoichiometry of staphylococcal  $\alpha$ -hemolysin in crystals and on membranes: a heptameric transmembrane pore. *Proc. Natl. Acad. Sci. USA* **91**:12828–12831.
- Guyonnet, F., and M. Plommet. 1970. Gamma hemolysin of *Staphylococcus aureus*: purification and properties. *Ann. Inst. Pasteur* **118**:19–33.
- Kamio, Y., A. Rahman, N. Nariya, T. Ozawa, and K. Izaki. 1993. The two staphylococcal bi-component toxins, leukocidin and gamma-hemolysin, share one component in common. *FEBS Lett.* **321**:15–18.
- Laemmli, U. K. 1970. Cleavage of structural proteins during the assembly of the head of bacteriophage T4. *Nature* **227**:680–685.
- Matsudaira, P. 1987. Sequence from picomole quantities of proteins electrophoretically onto polyvinylidene difluoride membranes. *J. Biol. Chem.* **262**:10035–10038.
- Miles, G., L. Movileanu, and H. Bayley. 2002. Subunit composition of a bicomponent toxin: staphylococcal leukocidin forms an octameric transmembrane pore. *Protein Sci.* **11**:894–902.
- Noda, M., T. Hirayama, I. Kato, and F. Matsuda. 1980. Crystallization and properties of staphylococcal leukocidin. *Biochim. Biophys. Acta Biochem. Biophys. Acta* **633**:33–44.
- Olson, R., H. Nariya, K. Yokota, Y. Kamio, and E. J. Gouaux. 1999. Crystal structure of staphylococcal LukF delineates conformational changes accompanying formation of a transmembrane pore. *Nat. Struct. Biol.* **6**:134–140.
- Pedelacq, J. D., L. Maveyraud, G. Prevost, L. Baba-Moussa, A. Gonzalez, E. Courcelle, W. Shepard, H. Monteil, J. P. Samama, and L. Mourey. 1999. The structure of a *Staphylococcus aureus* leukocidin component (LukF-PV) reveals the fold of the water-soluble species of a family of transmembrane pore-forming toxins. *Structure* **7**:277–287.
- Prevost, G., G. Cribier, P. Couppie, P. Petiau, G. Supersac, V. Finck-Barbancon, H. Monteil, and Y. Piemont. 1995. Panton-Valentine leukocidin and gamma-hemolysin from *Staphylococcus aureus* ATCC 49775 are encoded by distinct genetic loci and have different biological activities. *Infect. Immun.* **63**:4121–4129.
- Song, L., M. R. Hobaugh, C. Shustak, S. Cheley, H. Bayley, and J. E. Gouaux. 1996. Structure of staphylococcal  $\alpha$ -hemolysin, a heptameric transmembrane pore. *Science* **274**:1859–1866.
- Sugawara, N., T. Tomita, and Y. Kamio. 1997. Assembly of *Staphylococcus aureus*  $\gamma$ -hemolysin into a pore-forming ring-shaped complex on the surface of human erythrocytes. *FEBS Lett.* **410**:333–337.
- Sugawara, N., T. Tomita, T. Sato, and Y. Kamio. 1999. Assembly of staphylococcal leukocidin into a pore-forming ring-shaped complex on rabbit erythrocytes and human polymorphonuclear leukocytes. *Biosci. Biotechnol. Biochem.* **63**:884–891.
- Supersac, G., G. Prevost, and Y. Piemont. 1993. Sequencing of leukocidin R from *Staphylococcus aureus* P83 suggests that staphylococcal leukocidins and gamma-hemolysin are members of a single, two-component family of toxins. *Infect. Immun.* **61**:580–587.
- Tomita, T., D. Ishikawa, T. Noguch, E. Katayama, and Y. Hashimoto. 1998. Assembly of flammutoxin, a cytolytic protein from the edible mushroom *Flammulina velutipes*, into a pore-forming ring-shaped oligomer on the target cell. *Biochem. J.* **333**:129–137.
- Tomita, T., and Y. Kamio. 1997. Molecular biology of the pore-forming cytolytic toxins from *Staphylococcus aureus*,  $\alpha$ - and  $\gamma$ -hemolysins and leukocidin. *Biosci. Biotechnol. Biochem.* **61**:565–572.
- Woodin, A. M. 1960. Purification of the two components of leukocidin from *Staphylococcus aureus*. *Biochem. J.* **75**:158–165.